Materials Research, Vol. 10, No. 2, 177-181, 2007

Sol-Gel SiO_2-CaO-P_2O_5 Biofilm with Surface Engineered for Medical Application

Sonia Regina Federman[a]*, *Vilma Conceição Costa*[b], *Daniela Cordeiro Leite Vasconcelos*[c], *Wander Luiz Vasconcelos*[c]

[a]*Instituto Nacional da Propriedade Industrial – INPI, Av. Amazonas 1909, 30180-092 Belo Horizonte - MG, Brazil*
[b]*Fundação Centro Tecnológico de Minas Gerais, Av. Cândido da Silveira, 2000, 31170-000 Belo Horizonte - MG, Brazil*
[c]*Departamento de Engenharia Metalúrgica e Materiais, UFMG, Rua Espírito Santo, 35, s/206, Centro, Belo Horizonte - MG, Brazil*

Received: February 6, 2007; Revised: May 31, 2007

Sol-gel film in the SiO_2-CaO-P_2O_5 system was prepared from TEOS, TEP, alcohol and hydrated calcium nitrate in an acidic medium. The coatings were deposited on stainless steel using the dip-coating technique. After deposition, the composite was submitted to heat treatment, at different temperatures and exposure times to investigate the influence of such parameters on the surface morphology of the composite. The coated surfaces were characterized by AFM, SEM and FTIR. The present study showed that the formation of different textures (an important parameter in implant fixation) could be controlled by temperature and time of heat treatment.

Keywords: *coatings, biofilm, sol-gel, surface*

1. Introduction

The increase in the average lifespan of a human being, brought about by continuous improvements in the quality of modern life, is directly associated with the progressive deterioration of the musculoskeletal system. To keep the quality of life, scientists have been constantly searching for materials, which are able to repair defects, correct deformities, and replace damaged tissues[1-5].

A great number of materials are used today to replace damaged bones and tissues, including metallic materials due to their excellent mechanical properties, such as strength and hardness. Unfortunately, these materials have two main disadvantages: 1) the tendency to release metallic ions when exposed to body fluids and 2) the formation of a non-adherent fibrous capsule around implant[6-10]. Considering these disadvantages, ceramic materials (bioactive materials) have been successfully used to coat metallic materials for decades. Literature[1,5,6,11,12] shows that the importance of ceramic materials is due largely to their excellent behavior against corrosion and its capacity to spontaneously bond to and integrate with bones in the living tissue.

The sol-gel method involves hydrolyzing an alkoxide to produce a sol, which then undergoes policondensation to form a gel. This process allows one to engineer multicomponent oxide systems on a molecular level and manipulate process parameters to achieve desired products with specific properties. This process is characterized by hydrolysis, condensation reactions, as well as its potential to apply a uniform coating on complex shapes using different methods, including dip-coating, spin-coating and spray[13-15]. Because of its low processing temperature, higher purity, and homogeneous materials, the sol-gel method has been intensely studied as an alternative process for preparing ceramic and glass materials for a wide variety of applications, such as in the field of bioceramics (bioactive glass)[13,16-18].

The high specific surface area is beneficial toward medical applications as it can accelerate surface reactions and promote the growth of living tissue. The larger the surface area is, the larger the reactivity of the material. It has been reported on the literature[19-22] numerous methods used to improve the surface area, such as pore control and the use of mechanical equipment pressed against the surface, which is coated with a thin layer to form protuberances, which in turn will act as the sites promoting implant/tissue interaction.

Therefore, the aim of this study is to prepare a SiO_2-CaO-P_2O_5 biofilm whose surface area could be determined using a sol-gel route. The as-prepared solution was used to coat stainless steel with the intention of exploring its mechanical properties for a bioprothesis application. In this manner, the final composite could then be advantageously and successfully applied as a biomaterial implant.

2. Materials and Methods

Prior to coating, to improve the adhesion of films on metal surfaces, the metal surface must be prepared. In the present study, the sample, a stainless steel AISI 409, was cut in pieces of 2.0 x 2.0 cm, polished until 600 mesh to a higher surface finishing, washed with detergent, deionized water, and degreased with acetone. Finally, the sample was placed in an ultrasonic bath with acetone and dried in hot air.

The ternary film SiO_2-CaO-P_2O_5 preparation synthesis followed similar procedure to one used by Zhong et al.[23] and was as follows: the solution was prepared by mixing water, ethanol, and nitric acid, followed by the addition of TEOS (tetraethyl orthosilicate), TEP (triethylphosphate) and tetra hydrated calcium nitrate. Subsequently, the solution obtained was vigorously stirred for at least 50 minutes. The initial pH of the solution was 2 and the molar ratio of TEOS: H_2O: TEP: Ca = 1: 4: 0.03: 0.08. After stirring the mixed solution at room temperature the as-prepared solution was ready to coat. The substrate was lowered into the coating solution and withdrawn at speeds ranging between 3 and 5 cm/min at room temperature to ensure the elimination of organic residues as well as to develop a thin film. Following the deposition, samples were transferred to an oven for curing, using two heating schedules to set and solidify the SiO_2-CaO-P_2O_5 biofilm: a) the temperature was maintained at 200 °C

*e-mail: federman@inpi.gov.br

and the time processing changed from 15 minutes to 1 hour; b) the time processing was maintained at 15 minutes and the temperature increased to 400 °C. After heat treatment, the samples were removed from the oven to cool in open air, at which time the coating was found to be clear and free of any visible defects.

FTIR spectroscopy was employed to register the presence of specific chemical groups on the deposited SiO_2-CaO-P_2O_5 biofilm. A Variable Angle Specular Reflectance (VASR) accessory was used and the angles of incidence were 75°, 45°, and 25°. The variation of the incidence angle in the infrared spectroscopy allows an investigation of the film in layers of depth. The spectra were recorded between 4000 and 400 cm^{-1}, with a 4 cm^{-1} resolution and 64 scans.

The surface topography of the sol-gel derived thin films on stainless steel was investigated, at room temperature, with an atomic force microscope (Shimadzu Scanning Probe Microscope, SPM-9500-J3). Images were taken in dynamic tapping mode and the establishment of profile of roughness was done using the online application software, program licensed for SPM-9500 series.

Raman spectra were collected, at room temperature, in backscattering geometry using a Jobin Yvon/Horiba (model LABRAM-HR 800) instrument. An He-Ne laser (20 mW) was employed as the exciting radiation. Experimental conditions included 10 to 120 seconds for acquisition time.

Sol-gel ternary film surface morphology was analyzed by scanning electron microscopy (SEM) (JEOL, JSM-6360LV), using a secondary electron detector. Prior to SEM analysis, the surface sample was carbon coated to reduce charging in the samples.

3. Results and Discussion

Figure 1 shows the infrared spectra of three sol-gel heat treated films at 200 °C for 15 minutes in the range of 1500 to 400 cm^{-1}, obtained with a 75° angle of incidence. Figure 1 shows: a) unary film (only SiO_2), b) binary film (SiO_2-CaO) and c) ternary film SiO_2-CaO-P_2O_5. The first two a) and b), obtained in the same manner and under the same conditions as the SiO_2-CaO-P_2O_5, are illustrated only to point out the differences between the unary and binary films when compared to the ternary biofilm. Comparing the three spectra, it can be seen that the peak around the 1050 cm^{-1}, in the unary film which is associated with the transverse optical vibration mode corresponding to the asymmetric stretching of the intertetrahedral oxygen atoms in the Si-O-Si linkage[24-26], had in fact shifted toward larger wavenumbers (~1060 cm^{-1}) in the ternary film. This shift has been associated to the incorporation of phosphorus into the unary sol-gel film[27,28]. In addition, on the binary film, the addition of phosphorus also led to a shift in the Si-O-Si band from 1050 to 1060 cm^{-1}, as illustrated in Table 1.

Figure 1b and c, show additional weak bands located around 1420-1340 cm^{-1}. These bands are assigned to the presence of the nitrate group on the film structure[29,32]. However, these peaks are absent in the unary film, as shown in fig. 1a. The peak located around 932 cm^{-1} (unary film), attributed to the stretching vibrations of SiOH or SiO^- groups[26,33,34], shifted toward a large wavenumber (~938 cm^{-1}) in the ternary film; its intensity, however, decreased. It is important to recognize that the peak of around 1238 cm^{-1}, which has been attributed to the corresponding longitudinal optical (LO) vibration mode of the Si-O-Si linkage[24,35] in Figure 1, has the highest intensity, because of the large angle of incidence used, which is in accordance with that reported in prior literature[24]. For the ternary films the bands at the 900-1200 cm^{-1} range were attributed to the Si-O and P-O stretching vibrations. Literature shows that there is a superposition of bands located close to one another[34,36].

As can be seen in Figure 2, when a small incident angle (25°) was used in the FTIR experiment, the peak located around 1230 cm^{-1} diminished its intensity, which supports that reported in the literature for all three spectra[23]. It is clear that the nitrate group is also present on

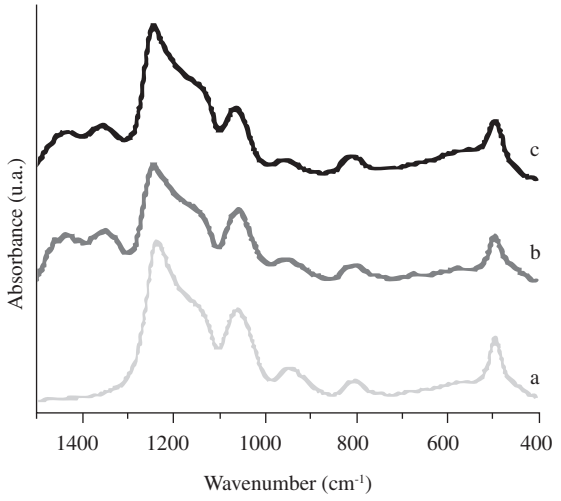

Figure 1. FTIR spectra of a) unary film; b) binary film; c) ternary film at 200 °C for 15 minutes at 75° of incidence.

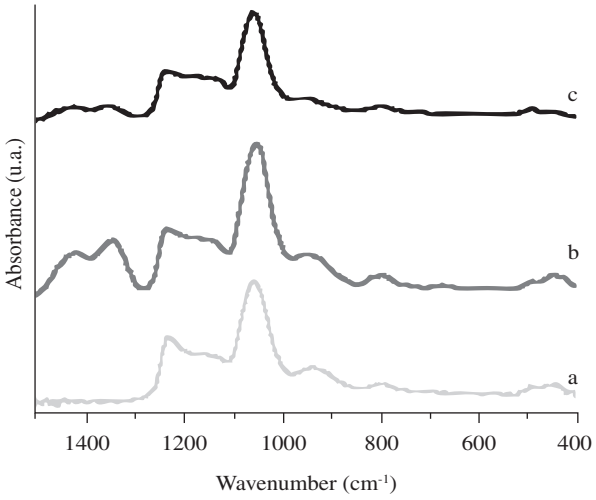

Figure 2. FTIR spectra of a) unary film; b) binary film; c) ternary film at 200 °C for 15 minutes at 25° of incidence.

Table 1. Shift in the Si-O-Si peak (cm^{-1}) caused by addition of phosphorous in unary, binary, and ternary sol-gel films.

Sol-Gel film	200 °C, 15 minutes			200 °C, 1 hour			400 °C, 15 minutes			400 °C, 1 hour		
	75°	45°	25°	75°	45°	25°	75°	45°	25°	75°	45°	25°
Unary	1050	1052	1052	1048	1050	1044	1046	1046	1046	1048	1042	1044
Binary	1050	1048	1045	1050	1049	1047	1036	1026	1024	1036	1032	1032
Ternary	1060	1054	1052	1052	1052	1050	1054	1048	1050	1054	1052	1052

the inner layer next to the substrate of SiO_2-CaO-P_2O_5 and SiO_2-CaO sol-gel films. Comparing Figures 1 and 2, one can observe that the intensity of the peaks due to calcium nitrate tends to diminish, from the external surface (Figure 1c) to the inner surface (Figure 2c).

Figure 2 also illustrates the presence of the nitrate group located at 1408-1342 cm^{-1} in the inner layer, next to the metallic substrate. Comparing the spectra (c) in Figures 1 and 2, we can consider that as the intensity of peaks located around 1408-1342 cm^{-1} tends to diminish from the external surface (75°) to the inner surface (25°), in the case of the ternary film, when using the incidence angle of 25°, it is possible to observe a tendency of decreasing the amount of nitrate groups on the inner layer of the film. Another important feature of the SiO_2-CaO-P_2O_5 film is that the intensity of the peak located at 938 cm^{-1}, due to its Si-OH / Si-O-Ca vibration mode[35], tends to diminish in comparison with unary and binary sol-gel films. This result suggests that the change in this band is attributed to P-containing species[33,35].

Table 1 presents the results obtained after the phosphorous species have been added to the unary and binary sol-gel films. In the case of the ternary film (the aim of this work), it is clear that the addition of phosphorous on unary or even on binary sol-gel film tends to cause a shift from peaks near 1050 cm^{-1} toward higher wavenumbers for any heat treatment at any schedule of temperature and at any part of the layer (75°, 45° or 25°). Another feature to point out is that peaks assigned to Si-O-Si asymmetric stretching (~1050 cm^{-1}) tend to shift slightly to lesser wavenumber, when moving from the external surface to the inner surface of the ternary film. This can be correlated with decreasing inorganic network density of this ternary film from the external to the inner surface.

Figure 3 illustrates the SiO_2-CaO-P_2O_5 sol-gel film which was heat treated at 200 °C for 1 hour. Peaks due to nitrate groups are still present on the external layer of the ternary film. However, as shown in Figure 4, for the ternary film (Figure 4c) heat treated at 400 °C for 15 minutes, one can observe the absence of relative absorption bands due to the nitrate groups (~1408-1342 cm^{-1}). These peaks are still present, but only on the binary film (Figure 4b), suggesting that the heat treatment of the films at 400 °C for at least 15 minutes leds to the decomposition of the nitrate residue on the film surface[24,37,38].

When calcium nitrate is decomposed by heat treatment at 400 °C for 15 minutes, calcium ions remain present in the silica network, as illustrated in Figure 5. Figure 5 is a Raman spectrum of the SiO_2-CaO-P_2O_5 film and shows a peak located at 1090 cm^{-1} (stretching vibration) assigned to calcium carbonate[39,40]. Figure 5 also illustrates the absence of peaks around 1046 cm^{-1}, assigned to the symmetric stretching of the nitrate groups. The absence of this absorption band confirms the total decomposition of the nitrate[31,39]. An additional peak, in Raman spectrum, appears near 720 cm^{-1} and is also assigned to carbonate groups[41].

The results shown up to now are in accordance with Figures 6 to 9. Figure 6 presents AFM image of samples coated with SiO_2-CaO-P_2O_5 biofilm, which was heat treated at 200 °C for 15 minutes. The AFM image shows distinct protuberances, which we suspect to be due to calcium nitrate, consequently raising the surface area of the sol-gel ternary film. In Figure 7, the AFM image of the sol-gel ternary film heated at 200 °C for 1 hour is shown. From this image, it can be observed that the protuberances on the ternary biofilm surface decreased and its appearance changed.

When the temperature of the heat treatment was changed to 400 °C, maintaining the time (15 minutes), the density and size of protuberances on the ternary biofilm drastically diminished on its surface, as illustrated in Figure 8. Changing the time processing to 1 hour while the temperature of 400 °C was maintained resulted in a low roughness surface.

Another important SiO_2-CaO-P_2O_5 biofilm feature to be emphasized from the AFM images is that the obtained ternary film conforms

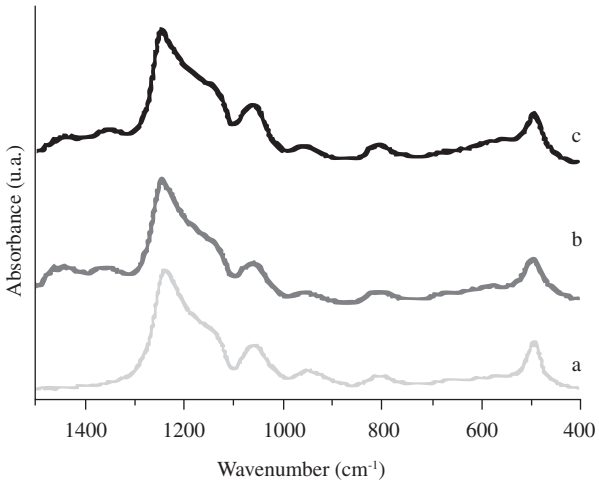

Figure 3. FTIR spectra of a) unary film; b) binary film; c) ternary film at 200 °C for 1 hour at 75° of incidence.

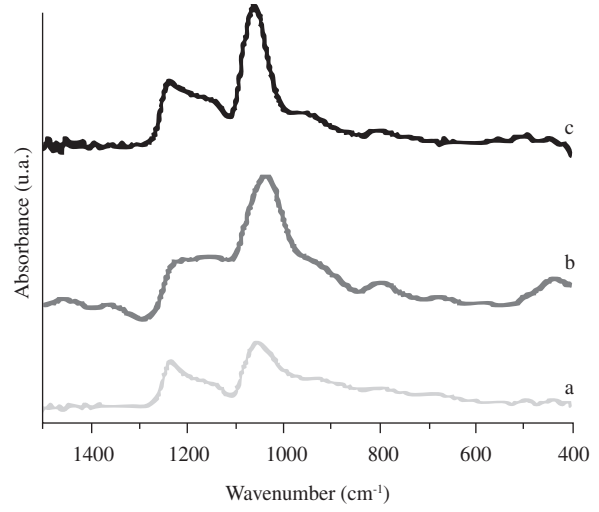

Figure 4. FTIR spectra of a) unary film; b) binary film; c) ternary film at 400 °C for 15 minutes at 75° of incidence.

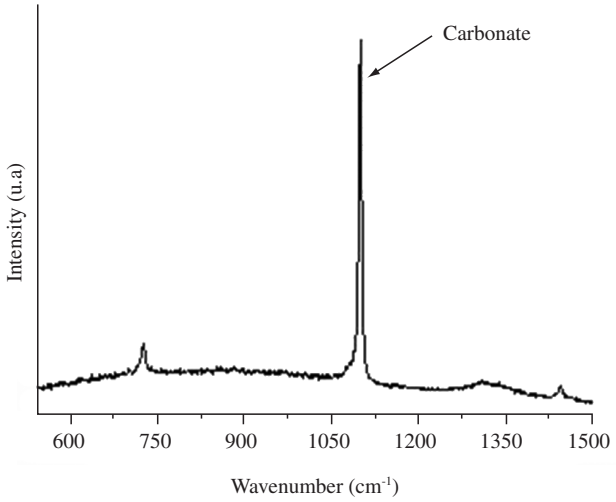

Figure 5. Raman spectrum of ternary sol-gel film heat treated at 400 °C for 15 minutes.

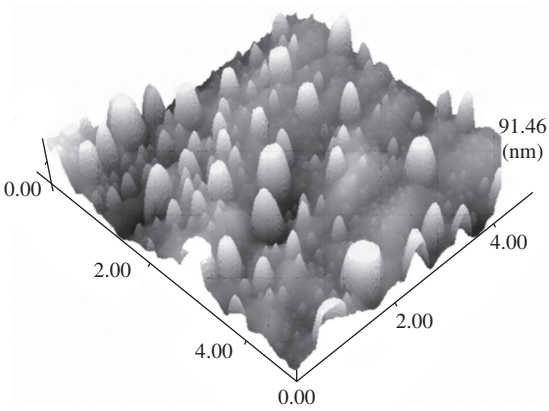

Figure 6. AFM image of ternary SiO_2-CaO-P_2O_5 film heated at 200 °C for 15 minutes.

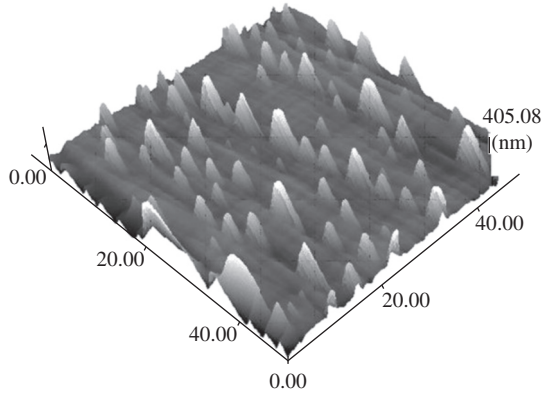

Figure 7. AFM image of ternary SiO_2-CaO-P_2O_5 film heated at 200 °C for 1 hour.

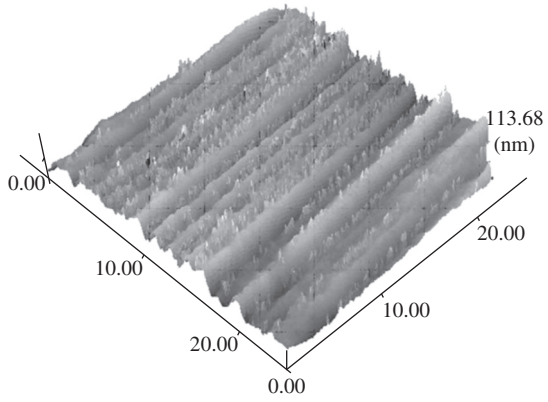

Figure 8. AFM image of ternary SiO_2-CaO-P_2O_5 heated at 400 °C for 15 minutes.

closely to the metallic surface. In the analyzed area through AFM, there is no suggestion of the macropores presence, cracks or any peelings from the substrate. Moreover, Figures 6 to 9 suggest that just as obtained ternary biofilm has a very small thickness, as can be seen from the parallel grinding lines beneath the SiO_2-CaO-P_2O_5 biofilm.

Figure 10 shows the SEM micrograph of the obtained SiO_2-CaO-P_2O_5 biofilm coated substrate, heat-treated at 200 °C. This result is

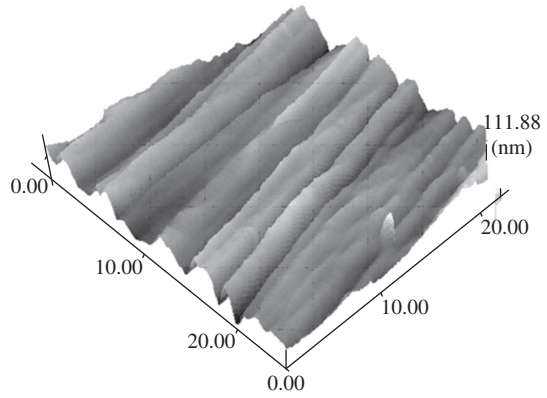

Figure 9. AFM image of ternary SiO_2-CaO-P_2O_5 heated at 400 °C for 1 hour.

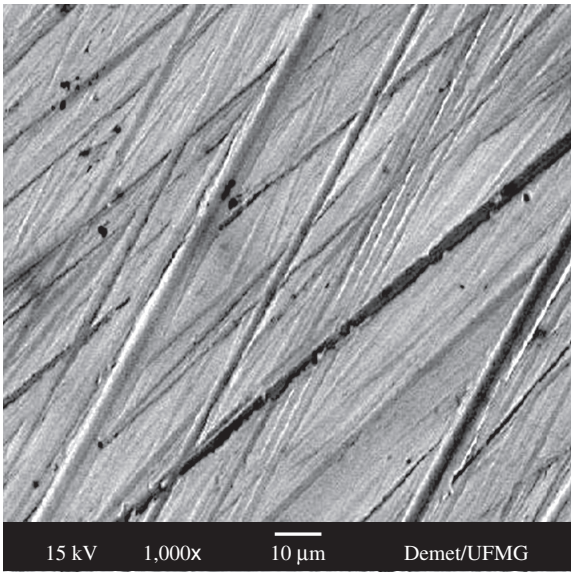

Figure 10. SEM micrograph of obtained SiO_2-CaO-P_2O_5 biofilm coated substrate at 200 °C.

in accordance with Figures 6 to 9 where, once again, the integrity of the ternary film can be seen, through of its strong adherence with the substrate.

4. Conclusion

The present study shows that it is possible to obtain a thin, uniform, pore/crack-free ternary biofilm in the SiO_2-CaO-P_2O_5 system using the sol-gel method. It also indicates that the biofilm topology can be altered, in relation to the presence (or absence) of protuberances, simply by changing the processing time and the temperature with the aim of designing its surface area.

Acknowledgments

The authors acknowledge Dr. Maria Silvia Sylva Dantas for Raman measurement and financial support from Minas Gerais Foundation of Research (Fapemig) and CNPq for financial support on this project.

References

1. Kawachi EY, Bertran C, Reis RR, Alves OL. Biocerâmica: Tendências e Perspectivas de uma área Interdisciplinar. *Química Nova*. 2000; 23(4):518-522.
2. Vallet-Regí M. Ceramics for Medical Applications. *Journal of the Chemical Society Dalton Transactions*. 2001; 2:97-108.
3. Ducheyne P, Radin S, Santos EM, inventors. University of Pennsylvania, assignee. *Incorporation of biological molecules into bioactive glasses*. US Patent 5874109; 1999 Feb 23.
4. Heimann RB. Materials Science of Crystalline Bioceramics: A review of Basic Properties and Applications. *CMU Journal*. 2002; 1:23-46.
5. Kokubo T, Kim HM, Kawashita M. Novel Bioactive materials with different mechanical properties. *Biomaterials*. 2003; 24:2161-2175.
6. Galliano P, Damborenea JJ, Pascual MJ, Durán A. Sol-Gel Coatings on 316L Steel for Clinical Application. *Journal of Sol-Gel Scienci and Technology*. 1998; 13:723-727.
7. Niedhart C, Sax HM, Niethard FU, Telle R, inventors. *Bioactive implants and method for the production thereof*. US Patent 6818332; 2004 Nov16.
8. Beloti MM, Rollo JMDA, Itman Filho A, Rosa AL. In vitro biocompatibility of duplex stainless steel with and without 0.2% niobium. *Journal of Applied Biomaterials & Biomechanics*. 2004; 2:162-168.
9. Durán A, Conde A, Gómez Coedo A, Dourado T, Garcia C, Ceré S. Sol-Gel Coatings for Protection and Bioactivation on Metal Used in Orthopaedic Devices. *Journal of Material Chemisty*. 2004; 14:2282-2290.
10. Moritz N, Rossi S, Vedel E, Tirri T, Ylänen H, Aro H, et al. Implants Coated with Bioactive glass by CO_2-laser, na in vivo study. *Journal of Material Scienci: Mater. in Medicine*. 2004; 15:795-802.
11. Rigo ECS, Oliveira LC, Santos LA, Bosh AO, Carrodeguas RG. Implantes Metálicos recobertos com Hidroxiapatita. *Revista Brasileira de Engenharia Biomédica*. 1999; 15(1-2):21-29.
12. Goetz M, Hotz W, Keppner H, inventors. Alusuisse Lonza Service, assignee. *Coating Substrate*. US Patent 6124039; 2000 Sept 26.
13. Balamurugan SK, Rajeswari S. Bioactive Sol-Gel Hydroxyapatite surface for Biomedical Application – *in vitro* study. *Trends in Biomaterial Artificial Organs*. 2002; 16(1):18-20.
14. Izquierdo-Barba I, Vallet-Regi M. The role of precursor concentration on the characteristics of SiO_2-CaO films. *Journal of Non-Crystalline Solids*. 2003; 26:1179-1182.
15. Mc Donagh C, Sheridan F, Butler T, MacCraith BD. Characterization of sol-gel- derived silica film. *Journal of Non-Crystalline Solids*. 1996; 194:72-77.
16. Hench L L, Wilson J, editors. *An introduction to bioceramics*. Florida. World Scientific; 1993. p. 386.
17. Saravanapavan P, Hench L. Low-temperature synthesis, structure, and bioactivity of sol-gel derived glasses in the binary CaO-SiO_2 system. *Journal of Biomedical Material Research*. 2001; 54:608-618.
18. Beganskiené A, Dudko O, Surytjautusm R, Giraitis R. Water based sol-gel synthesis of hydroxyapatite. *Materials Science*. 2003; 9(4):383-386.
19. Tsutomu M, Tatsumisago, Tadanaga K, Matsuda A, Hori M, Nakamura K, et al., inventors. *Article having a predetermined surface shape and method for preparation thereof*. US Patent 6849350; 2005 Feb 1.
20. Katsuhide S, Kenichi N, inventors. Nippon Sheet Glass Co., assignee. *Article having uneven surface, production process for the article, and composition for the process*. US Patent 6361718; 2002 Mar 26.
21. Katayama S, Yamada N, Awano M. Preparation of silicate foams using HSi $(OC_2H_5)_3$; and their NO_x adsorption behavior. *Journal of European Ceramic Society*. 2004; 24:1957-1960.
22. Hall S R, Dominic W, Green D, Oreffo R, Mann S. A novel route to highly porous bioactive silica gels. *Journal of Material Chemical*. 2003; 13:186-190.
23. Zhong J, Greenspan D C, inventors. US Biomaterials Corp., assignee. *Bioactive sol-gel compositions and method*. US Patent 6171986; 2001 Sept 01.
24. Primeau N, Vautey C, Langlet M. The effect of thermal annealing on aerosol-gel deposited SiO_2 films: a FTIR deconvolution study. *Thin Solid Films*. 1997; 310:47-56.
25. Zarzosa-Ortega G, Martinez JR, Espinós-Dominguez O, Ruiz F, Matutes-Aquino JA. Formation of copper-based particles trapped in a silica xerogel matrix. *Superficies y Vacio*. 2000; 11:61-65.
26. Viitala R, Jokinen M, Maunu SL, Jalonen H, Rosenholm JB. Chemical characterization of bioresorbable sol-gel derived SiO_2 matrices prepared at protein-compatible pH. *Journal of Non-Crystalline Solids*. 2005; 351:3225-3234.
27. Ahsan R Md, Mortuza JG. Infrared spectra of $xCaO(1-x-z)SiO_2$ zP_2O_5 glasses. *Journal of Non-Crystalline Solids*. 2005; 351:2332-2340.
28. Solla EL, Borrajo JP, González P, Serra J, Liste S, Chiussi S. et al. Plasma assisted pulsed laser deposition of hydroxyapatite thin film. *Applied Surface Science*. 2005; 248:360-364.
29. Miller FA, Wilkins CH. Infrared spectra and characteristic frequencies of inorganic ions – Their use in qualitative analysis. *Analytical Chemical*. 1952; 24(8):1253-1294.
30. Gladsten Aric JA. *Infrared spectra of minerals and related inorganic compounds*. 1975; ISBN 0408706651.
31. Briget MM, Sasirekha V, Ramakrishnan V. Plasma assisted pulsed laser deposition of hydroxyapatite thin film. *Spectrochimica Acta A*. 2005; 62:446-452.
32. Chouillet C, Krafft J M, Louis C, Lauron-Pernot H. Characterization of zing hydroxynitrates by diffuse reflectance infrared spectroscopy-structural modifications during thermal treatment. *Spectrochimica Acta Part A*. 2004; 60:405-511.
33. Fidalgo A, Ilharco LM. The defect structure of sol-gel-derived silca/polytetrahydrofuran hybrid films by FTIR. *Journal of Non-Crystalline Solids*. 2001; 283:144-154.
34. Cerruti M, Greenspan D, Powers K. Effect of pH ionic strength on the reactivity of Bioglass 45S. *Biomaterials*. 2005; 26:1665-1674.
35. Nitta SV, Pisupatti V, Jain A, Wayner PC, Jr W NG, Plawsky JL. Surface modified sping-on xerogel films as interlayer dielectrics. *Journal Vacio Science Technology B*. 1999; 17(1):205-212.
36. Szumera M, Waclawska I, Mozgawa W,Sitarz M. Spectroscopic study of biologically active glass. *Journal of Molecular Structure*. 2005; 744-747:609-614.
37. Saravanapavan P, Hench LL. Mesoporous calcium silicate glasses. I. *Synthesis Journal of Non-Crystalline Solids*. 2003; 318:1-13.
38. Laudisio, G, Branda F. Sol-gel synthesis and crystallization of $3CaO.2SiO_2$ glassy powders. *Thermochimica Acta*. 2001; 370:119-124.
39. Tang IN, Fung KH. Hydration and Raman scattering studies of levitated microparticles: $Ba(NO_3)_2$ and $Ca(NO_3)_2$. *Journal of Chemical Physics*. 1997; 106(5):1653-1660.
40. Edwards HGM, Villar SEJ; Jehlicka J, Munshi T. RT-Raman spectroscopy study of calcium-rich and magnesium-rich carbonate minerals. *Spectrochimica Acta Part A*. 2005; 61:2273-2280.
41. Simpson LJ. Electrochemically generated $CaCO_3$ deposits on iron studied with FTIR and Raman spectroscopy. *Electrochimica Acta*. 1998; 43(16-17):2543-2547.